Asian Journal of Physics
Vol. 25, No 3 (2016) 311-324
*Available on: www.asianjournalofphysics.in*

# Solar interior structure and dynamics

R Howe
*University of Birmingham, Edgbaston, Birmingham B15 2TT, United Kingdom*

Helioseismology allows us to probe the interior structure and dynamics of the Sun, and long-term observa-tions allow us to follow their temporal variations. This review describes the important findings of recent years, covering the interior structure, the near-surface changes related to the solar cycle and possible deeper-seated variations, the interior rotation profile, and solar-cycle related changes in the zonal and meridional flows. 
**Keywords**: Sun: Seismology; Sun: Interior; Sun: Rotation

## 1 Introduction

While the solar layers from the corona down to the photosphere can be directly observed using suitable instrumentation, the interior – everything that lies below the opaque photosphere – can only be observed by indirect methods. The most important of these methods in the last half-century has been helioseismology, in which the (mainly acoustic) waves that propagate through the solar interior are monitored at the surface in intensity or Doppler velocity and their frequencies are used to deduce the interior structure and dynamics. While the field of helioseismology recently celebrated its 50th anniversary, the past two decades have seen significant advances due to the availability of continuous, high-quality resolved-Sun observations from the Global Oscillation Network Group (GONG [1]) starting in 1995, from the Michelson Doppler Imager (MDI [2]), which launched onboard the *Solar and Heliospheric Observatory (SOHO)* in 1996 and observed until early 2011, and from the Helioseismic and Magnetic Imager (HMI [3]), which launched onboard the *Solar Dynamics Observatory (SDO)* in early 2010. There are also instruments dedicated to low-degree, 'Sun as a star' observations, such as the Birmingham Solar-Oscillations Network (BiSON [4, 5]) and the Global Oscillations at Low Frequencies (GOLF: [6]) instrument onboard SOHO, for example.

In this review we examine some of the important recent results. Section 2 covers the solar interior structure and its temporal variation, while Section 3 deals with the interior dynamics, including the rotation profile and the meridional circulation, together with their temporal variations.

## 2 Solar interior structure

### *2.1 Sound-speed and density stratification*

The term "structure" in the helioseismic context refers to properties of the solar interior such as sound-speed and density. Such quantities are inferred by inversion of the acoustic mode frequencies – usually, in practice, by the inversion of differences between the observed frequencies and those predicted by a particular model. In current models these differences are usually less than one part in a thousand, once the frequency-dependent 'surface term' has been removed, as seen for example in Fig 1. In this figure,'Model S' refers to a model by Christensen-Dalsgaard *et al* [9], which is popular with helioseismologists because its differences from the observations are small and show distinct features of interest, in particular the 'bump'

*Corresponding author :*
*e-mail : rhowe@noao.edu* (R Howe)

in the sound speed at the bottom of the convection zone due to the lack of turbulent diffusion in the model. The good agreement between standard solar models and observations implied that the solar neutrino problem – the discrepancy between the predicted and observed levels of neutrinos from the Sun detected on Earth– could not be a problem with the solar models [10]. However, subsequent changes to the solar element abundances [11], which yielded lower metallicity – lower abundances of heavy elements – resulted in much worse agreement between models and observations [12], which would require substantial adjustments to the opacity tables and/or other input physics to bring the models back into line with the observations. Much effort was subsequently expended on this problem [13] without much success. This led to the conclusion [13, 7] that the new, low-metallicity element abundances may be flawed and it would be better to use the earlier ones.

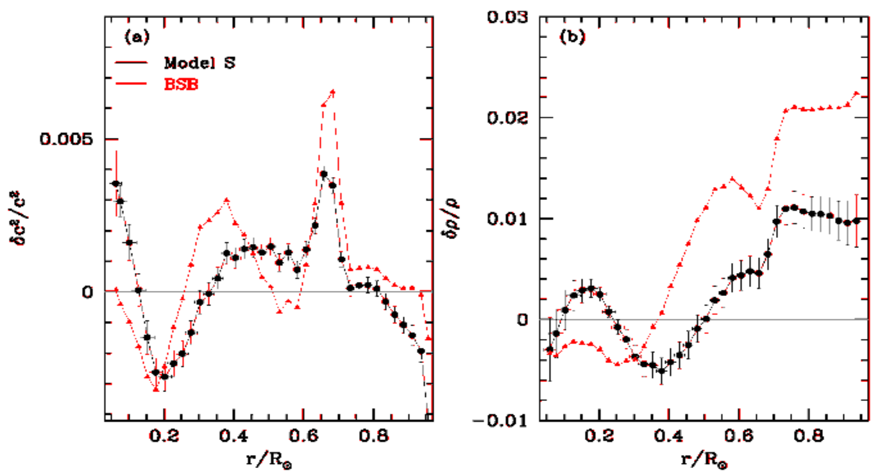


Fig 1. The relative differences of the squared sound speed between the Sun and two other solar models, Model S and model BSB. (b) The relative density differences between the Sun and the two models. The results, which were obtained by inverting the frequency differences between the Sun and these models, are from Basu *et al* (2009) [7]. Figure taken from Schmitt and Basu [8] by kind permssion of S. Basu

### *2.2 Temporal variations*

#### *2.2.1 Frequency shifts*

One of the early findings from systematic helioseismic observations was that the mode frequencies vary with the level of solar activity. The effect was seen [14] using unresolved-Sun observations from the ACRIM (Active Cavity Radiation Monitor) instrument; the frequency of the oscillations changed by about 0.5 microHz between 1981 (solar maximum) and 1984–5 (close to solar minimum.) The variation was later confirmed for low-degree modes in ground-based velocity observations from instruments of what would later be known as the BiSON network [15, 16], while Libbrecht and Woodard [17] found that the changes also occurred in resolved-Sun observations at the Big Bear Solar Observatory. These variations correlate with the distribution of surface magnetic activity in location as well as time for both medium-degree global modes [18, 19] and local modes [20, 21]. Figure 2 shows the variation of the central frequency of one ($l$, $n$) multiplet from GONG data, and Fig 3 shows the result of one-dimensional latitudinal inversions of the frequency shifts [19] for nearly 20 years of GONG observations, showing how the shifts map to the magnetic butterfly diagram. The frequency-dependence of these changes (with higher-frequency modes, at least below the acoustic cut-off frequency, responding more strongly to activity changes than lower-frequency modes [17, 22]) implies that the changes are confined to the near-surface layers of the Sun.

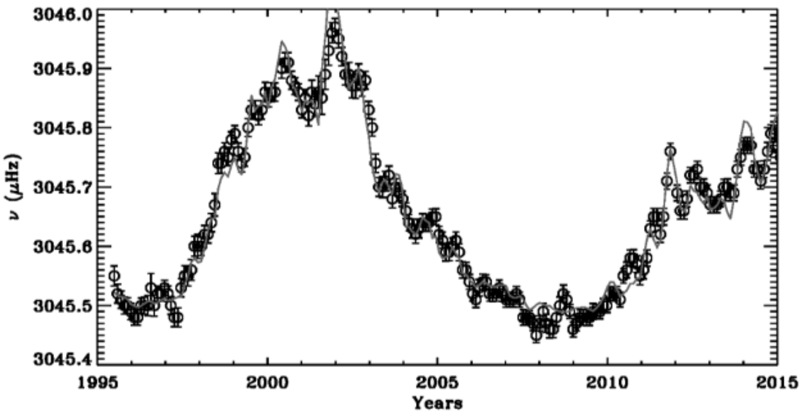


Fig 2. The central frequency of the $l = 50$, $n = 10$ multiplet over time, from GONG data. The solid curve represents the best linear fit to the 10.7 cm radio flux index.

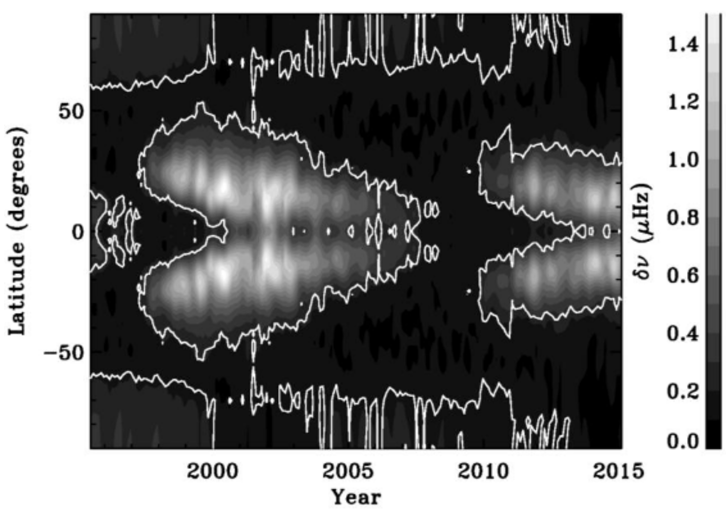


Fig 3. Mean frequency shifts for modes with $40 \leq l \leq 80$ and $9 \leq n \leq 11$ observed by GONG, inverted to show the latitudinal distribution [19]. The white contour indicates the 5G level of the unsigned magnetic field strength from Kitt Peak synoptic maps. Note that both the shifts and the magnetic data are symmetrized across the equator, as the global analysis does not allow us to distinguish the two hemispheres.

Various mechanisms have been proposed for the frequency changes. Many of these have invoked magnetic field effects at various depths, for example in the chromosphere [23, 24], the photosphere [25], the 50 Mm depth around which sunspots are anchored [26], or at the base of the convection zone [27]. An alternative explanation [28] attributes the shifts to changes in the physical size of the cavity in which the modes propagate; the question is not yet definitively settled, but it is widely accepted that the changes are mostly confined to the outer layers.

*2.2.2 Variations beyond the 11-year cycle*

Not all of the observed frequency shifts directly correlate with solar activity indices, and there have been reports in recent years that the relationship between shifts and activity may vary between solar cycles or between different phases of the cycle. While these may seem like two distinct phenomena, it is difficult to disentangle them, as a short-term variation may reduce the level of correlation between the frequencies and the activity index. For example, Basu *et al* [29] found that the trend extrapolated from the BiSON shifts in Cycle 22 did not match the shifts observed in Cycle 23, and interpreted this as evidence for thinning of the subsurface magnetic layer, while on the other hand Salabert *et al* [30], using GOLF data, found a larger frequency increase in Cycle 24 than would have been expected for a comparable activity level in Cycle 23. Such results may be quite sensitive to which modes are averaged and what is used as a reference.

The so-called quasi-biennial oscillation (QBO) in the low-degree frequencies was reported for example by Fletcher *et al* [31], who looked at frequency shifts from BiSON and GOLF and found that after subtracting the dominant 11-year cycle from the frequency shifts there remained a signal with a period of about two years that was strongest at solar maximum. Unlike the strongly frequency-dependent solar cycle effect, this oscillation has a similar amplitude at all frequencies. The authors suggest it may be related to a 'second solar dynamo' operating close to the surface, but the effect is still not well understood.

#### *2.2.3 Interior structure variation*

While the mode frequency changes are dominated by the near-surface layers, some attempts have been made to use helioseismology to probe structural changes deeper in the convection zone.

There have been some reports that the solar-cycle structure variation has a two-layer configuration. Lefebvre and Kosovichev [32] found a two-layer structure in the variation of the so-called 'acoustic solar radius' measured using MDI data; More recently Rabello-Soares [33], also using global analysis of MDI data, found a two-layer structure in the sound speed. A two-layer structure has also been commonly found in local helioseismic analysis of the sound-speed around active regions, but there are doubts about the reliability of this analysis, as the measurements are very prone to be affected by surface magnetic fields and give inconsistent results when applied to the same feature [34].

Some studies found indications of a solar-cycle change in the signature of the helium ionization zone at 0.98 $R_{SUN}$ in mode frequencies at medium [35] and low [36] degree. However, this result was not reproduced in more recent work [37].

Eff-Darwich *et al* [38] put an upper limit on any temporal variations of the interior sound speed at a fractional change of $3 \times 10^{-5}$. Baldner and Basu [39] found subtle solar-cycle changes in the structure at the base of the convection zone, just below the Eff-Darwich limit.

## 3 Solar interior dynamics

### *3.1 Rotation*

The Sun's rotation breaks its spherical symmetry and hence breaks the degeneracy between modes of the same radial order and degree but different azimuthal order ($m$), giving rise to rotational splitting. This makes it possible to map the interior rotation in two dimensions using inversion techniques. Two commonly used techniques are regularized least squares (RLS) [40] and optimally localized averages (OLA) [41, 42]. These represent different approaches to the problem of balancing noise and resolution. In the RLS approach we use a least-squares fit to minimize the difference between the observed splittings and those predicted from the inferred rotation profile; a smoothness constraint is included by adding a second-derivative term to the quantity to be minimized. The balance between noise and resolution is then controlled by empirically chosen trade-off parameters in the radial and latitudinal directions. In OLA, on the other hand, the inversion attempts to match the shape of the averaging kernel – the weighting function that relates the inferred rotation rate at a given location to the underlying rotation profile – to a predetermined form such a 2-dimensional Gaussian function. The effectiveness of the inversion technique is limited by the available modes; as depth below the surface increases there are fewer modes to contribute to the estimate, so the resolution decreases and the results become more vulnerable to errors in the input data. For more detailed discussion on solar rotation inversions, see the article by Schou *et al* [43] and the review by Howe [44].

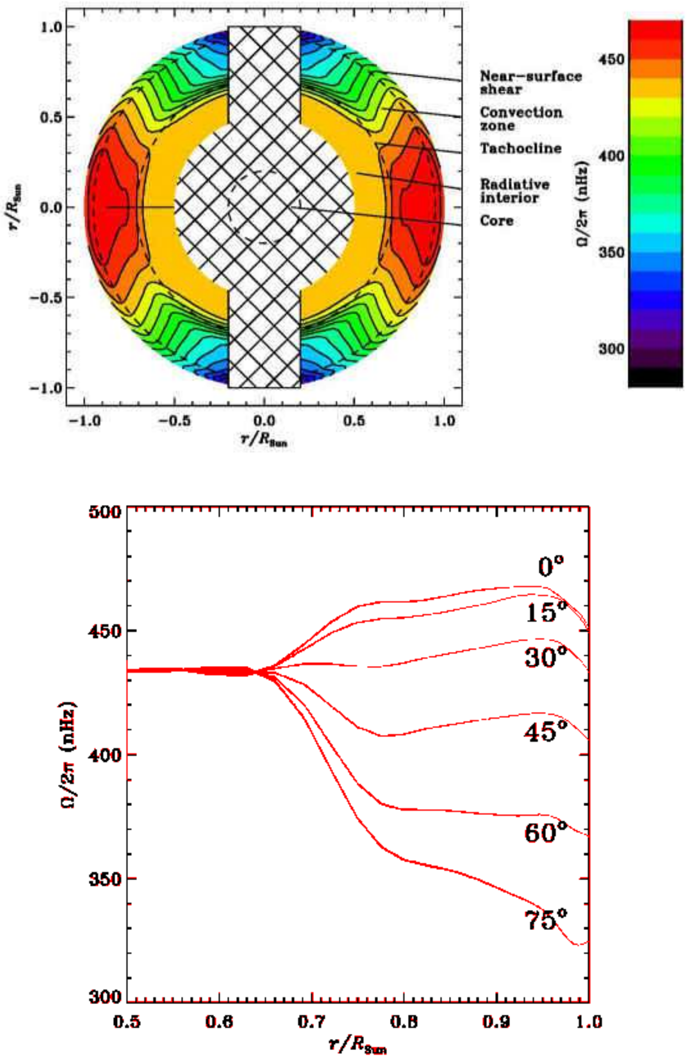


Fig 4. Features of the interior rotation, based on the mean of 19 RLS inversions of HMI data covering the period 2010 - 2014. Upper panel: contour map; lower panel: rotation rate as a function of radius at selected latitudes.

Figure 4 shows the solar interior rotation derived from 2d RLS inversions of data from HMI.

### *3.1.1 The core and the radiative interior*

Only the lowest-degree acoustic modes penetrate into the deep interior of the Sun, and even those modes are heavily weighted towards the outer layers. Although the low-frequency low-degree modes observed for example by BiSON are very sharp, they are also of low amplitude, while the higher-frequency low-degree modes are too broad for the rotational splitting (approximately 0.8 μHz between the $m = \pm 1$ components of the $l = 1$ mode) to be resolved. This means that in practice it is not possible to use the *p*-mode splittings to determine the rotation rate below about 0.2 $R_{SUN}$ [45], or to rule out the possibility that the core is rotating substantially faster than the radiative envelope [46]. A recent attempt to constrain the interior rotation using data from GONG, MDI, and HMI was made by Eff-Darwich *et al* [47]; they were still unable to rule out a fast- or slow-rotating core. In the radiative zone their results were consistent with rigid rotation at approximately 431 nHz; however, they report "a consistent and systematic dip in the rotation profile located at around 0.4 $R_{SUN}$ and 60 degrees of latitude."

If solar *g*-modes (waves in which the restoring force is gravity, and which have their highest amplitudes in the core) were readily observed, they would provide a much better way to constrain the core rotation. However, there are still no independently verified findings of *g*-modes in solar data, though the search continues. Unfortunately, it seems that such modes have very small amplitudes at the surface. One recent report was by García *et al* [48] based on GOLF observations, who found indications of a pattern of peaks consistent with $l = 2$ *g*-modes with a splitting corresponding to a core rotation rate three to five times higher than the surface rate.

### *3.1.2 The tachocline*

Between the rigidly rotating radiative interior and the differential rotation in the convection zone lies a region of strong radial shear known as the tachocline, which was first detected in helioseismic observations by Brown *et al* [49] and Dziembowski *et al* [50]. The shear is approximately centered on the bottom of the convection zone as determined from structure inversions, which is at 0.713 $R_{SUN}$ [51]. This region is not fully resolved in most inversions; while the inversion results seem to show a rather gentle slope occupying about 10% of the solar radius, this is largely an artifact of the limited resolution. Estimates of the true thickness of the tachocline range from 12% [52] based on splitting coefficients from the Big Bear Solar Observatory observations to 1% [53] based on a specialized inversion technique applied to data from the LOWL instrument. All of these estimates suggest a thinner tachocline than can easily be explained by simple models or even by detailed simulations [54]; the confinement of the tachocline is one of many puzzles in solar dynamics. The tachocline plays an important role in dynamo models of the solar cycle.

### *3.1.3 The convection zone*

In the bulk of the convection zone, the Sun's rotation is differential, with the slowest rotation near the poles and the fastest at the equator. Below about 0.95$R_{SUN}$ is almost but not quite constant on radial lines. In fact, over a wide range of latitudes the rotation contours lie at an angle of approximately 25 degrees to the rotation axis [55, 56], which may be due the Coriolis effect acting on the meridional circulation.

### *3.1.4 The near-surface shear*

In the upper layers of the convection zone, down to about 0.95 $R_{SUN}$, the rotation rate increases with depth. Because the *p*-modes used in global analysis do not resolve this region, the best way to study it is using the f modes. Corbard and Thompson [57] carried out such an analysis using *f*-mode data from MDI. They found that the logarithmic gradient, $d \ln \Omega / d \ln r$, had a value of −1 at low latitudes, whereas the standard understanding of momentum conservation would require a value of −2 [58]. They also found that the gradient decreased at latitudes above 30 degrees.

Barekat *et al* [59] confirmed the low-latitude result but obtained somewhat different results at higher latitudes using HMI data and more recently re-analyzed MDI data, with the sign of the near-surface shear remaining negative at least up to 60 degrees latitude. They concluded that the results above this latitude should be treated with caution as they are vulnerable to systematic error, and that the decrease in the gradient seen with the earlier MDI data may have been spurious.

### *3.1.5 Temporal variation*

The interior and near-surface rotation are not static, but change during the solar cycle. Howard and Labonte [60], using surface Doppler observations from the Mount Wilson observatory, first observed a pattern of bands of faster and slower rotation propagating from mid-latitudes towards the equator during the solar cycle, which they dubbed the 'torsional oscillation.' The first helioseismic detection of the flows was made in MDI f-mode data [61]. Within a few years, global p-mode data from MDI and GONG revealed that the flows penetrated a substantial distance – at least to $0.92R_{SUN}$ – below the surface [62-65]. As well as the bands moving towards the equator, at higher latitudes bands of faster rotation moves towards the poles [66]; this high-latitude branch appears to penetrate the full depth of the convection zone [65]. These patterns are revealed by subtracting a temporal mean at each depth and latitude from each of a series of 2-dimensional rotation inversions. The flow patterns found with global helioseismology correspond to those found using local helioseismic analysis [67].

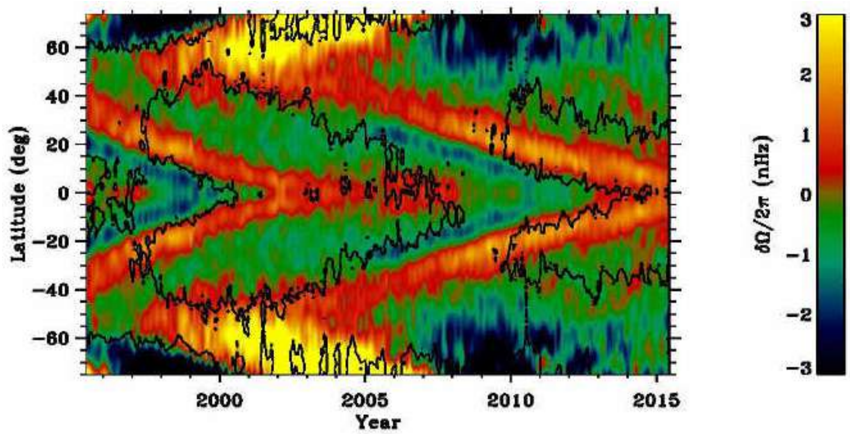


Fig 5. Zonal flow residuals from RLS inversions of GONG, MDI, and HMI data at 0.99 $R_{SUN}$. The black contour indicates the 5 G level of the unsigned magnetic flux from Kitt Peak synoptic maps.

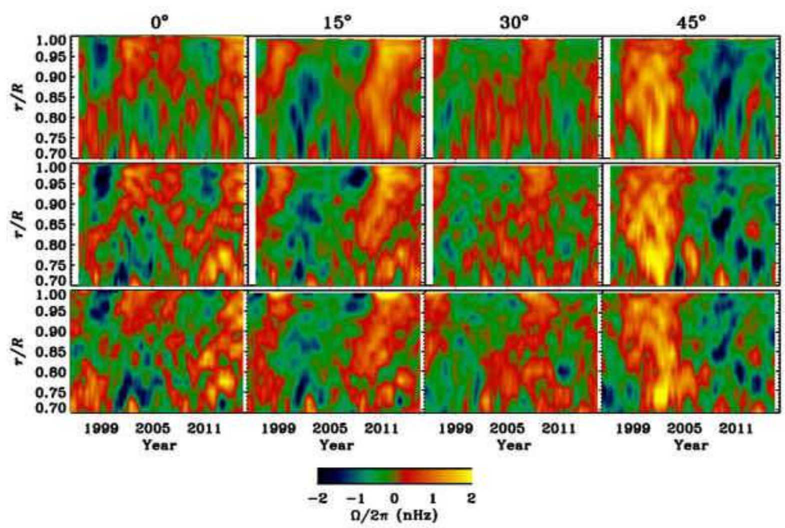


Fig 6. Time-radius plots of the rotation-rate residuals in the convection zone at selected latitudes (0, 15, 30, 45 degrees, from left to right), for OLA (top row) and RLS (middle row) inversions of MDI and HMI data, and for RLS inversions of GONG data (bottom row).

Figure 5 shows the near-surface flows from GONG, MDI, and HMI data, covering the period from the beginning of the GONG observations in 1995 to the most recent data available at the time of writing. Figure 6 shows the rotation residuals as time–radius maps at selected latitudes.

During Solar Cycle 23 (1996 – 2009) there were indications that either the flow pattern propagated radially upwards from the solar interior over about two years, or the flow belts had the same 25-degree inclination to the rotation axis as the rotation contours [56, 68]. Also, during this epoch the variation of the near-surface rotation at low and middle latitudes could be well described by a combination of an 11-year sine wave and its second harmonic [56]. However, during the unusually deep and extended solar minimum following Cycle 23 these patterns were less clear. The apparent length of the cycle, based on the best fit of a cycle and its second harmonic or on cross-correlation of the recent configuration of the flows with that in the previous cycle, gradually increased as the equatorward migration of the mid-latitude flow belt appeared to stall [69]. Only when the branch finally reached a latitude around 20 degrees in late 2009 did widespread solar activity return [70]. Meanwhile, the high-latitude branch for Cycle 24 is not evident on a map where the rotation rate subtracted is over the whole period of the observations. However, if the average is taken only over the rising phase of the new cycle a rather weak and disorganized high-latitude branch is seen, superimposed on a lower average rotation rate [71], as illustrated in Fig 7. This may be associated with the weaker polar magnetic fields in Cycle 24 [72].

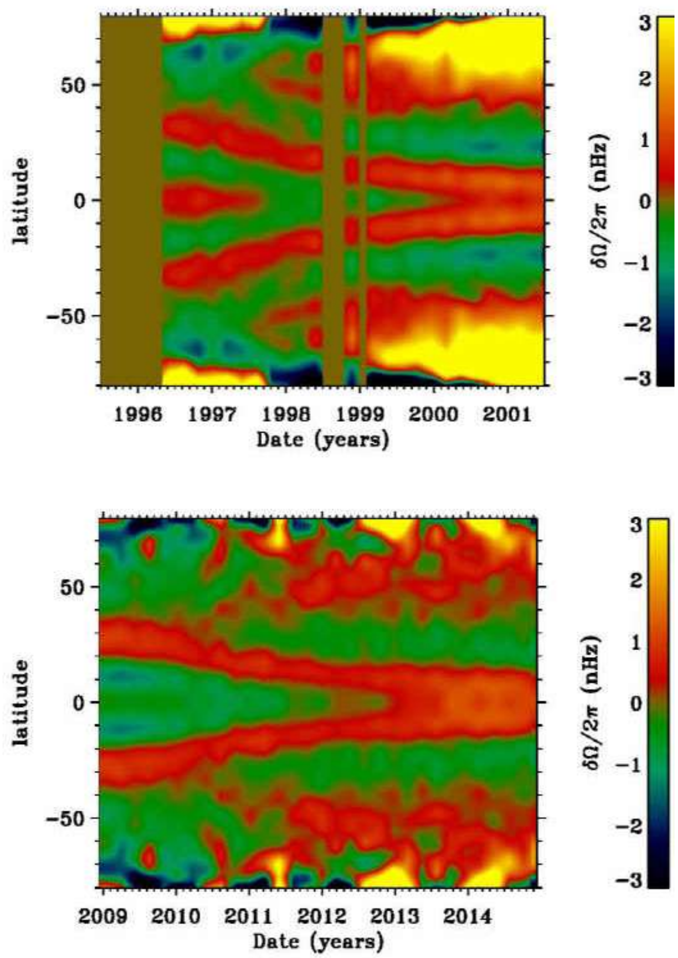


Fig 7. Near-surface zonal flow maps from OLA inversions of MDI and HMI data, for the ascending and maximum phases of Solar Cycle 23 (upper panel) and 24 (lower panel). The mean subtracted in each case was taken over the 3.5 years from solar minimum.

From a theoretical point of view, the torsional oscillation is generally considered as a kind of sideeffect of the magnetic field variation during the solar cycle. It has been modeled as a result of the Lorentz force due to dynamo waves [73, 74] and as a geostrophic flow associated with active regions [75]. None of these models appears entirely to account for the observed depth structure.

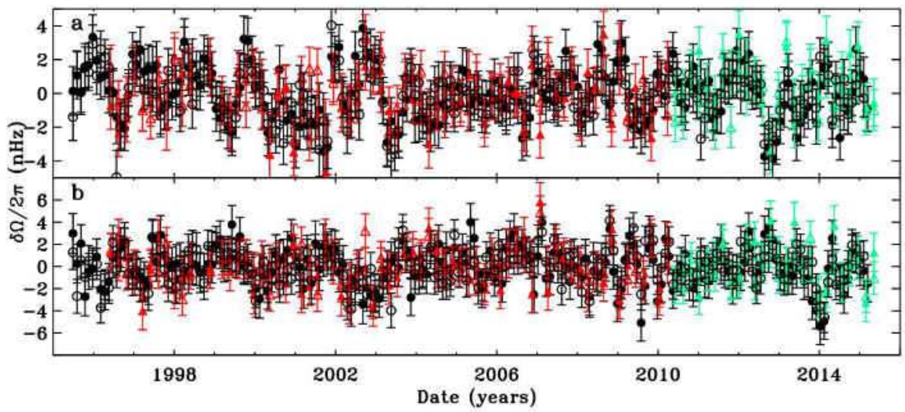


Fig 8. Variation of the rotation-rate residuals from RLS (filled symbols) and OLA (open symbols) analysis of GONG (black circles), MDI (red triangles), and HMI (green triangles) data at $0.72R_{SUN}$ (top) and $0.72R_{SUN}$ (bottom), just above and below the base of the convection zone. In the period 1995-2000 there appears to be an oscillatory signal with period 1.3 years.

Howe *et al* [76] reported an oscillatory signal in the rotation rate at the base of the convection zone in the first few years of GONG and MDI observations (see Fig 8). This was of interest because of the role of the tachocline in the dynamo and because signals of a similar period had been seen in some geophysical and heliospheric phenomena [78,79] However, the result was not reproduced by other authors analysing the same data [80]. The strong periodic signal disappeared in later years [81], although the observations from the different projects continued to fluctuate together [82].

### *3.2 The meridional flow*

The meridional flow from the equator towards the poles is a vital component of the solar cycle, as it carries the magnetic field from disintegrating active regions towards the poles and eventually causes the sign of the polar field to reverse. This flow cannot be measured by conventional global helioseismic techniques. In the outer layers of the convection zone it can be studied using local helioseismic techniques such as ring-diagram [83] and time-distance [84] analysis. These measurements are quite susceptible to systematic error, especially at high latitudes where projection effects become severe. There have been reports of 'counter-cells' (reversed direction of meridional flow) at high latitudes, for example by Haber *et al* [85] using MDI data, while González Hernández *et al* [86] found that in GONG data, which unlike MDI was available continuously throughout the year, the appearance of such cells was highly correlated with the solar B-angle, the angle of inclination of the solar rotation axis to the observer. Zaatri *et al* [87] proposed an ad-hoc correction to remove such variations.

Recently it was found that there is a 'center to limb' systematic effect, particularly in time-distance measurements [88], which affects both zonal and meridional flows away from disk center, producing a variation in the zonal flow with distance from the meridian and an additional change in the meridional flow with latitude. Because the effect is rotationally symmetric, the effect on the meridional flow can be corrected in an ad-hoc fashion if one assumes that the zonal flow should not vary with longitude. This effect appears to vary with the height in the atmosphere of the observable used for the analysis. One suggested explanation

[89] is that it is caused by the asymmetric nature of flows in granules.

*3.2.1 The deeper interior*

The meridional circulation in the deeper layers of the convection zone is still challenging to measure, but in recent years several attempts have been made to probe it.

Hathaway [90] inferred a return flow at a depth of 70 Mm (i.e, about 10% of the solar radius below the surface), by supergranule correlation tracking.

After correcting for the center-to-limb effect discussed above, Zhao *et al* [91], using time-distance analysis on two years of HMI data, found an equatorward flow in the middle of the convection zone and indications of a second poleward flow at greater depths, suggesting a two-cell structure that would challenge understanding of how magnetic field is transported within the convection zone. Independently and almost at the same time, Schad *et al* [92] analyzed MDI data using a global helioseismic technique involving the perturbations to global modes caused by the meridional flow, and found a complex multi-cell structure in the deeper parts of the convection zone. Kholikov *et al* [93], analyzing several years of GONG data, found indications of possible equatorward flow near the bottom of the convection zone and possible indications of a multiple-cell structure. On the other hand, Jackiewicz *et al* [94] analyzed two years of GONG data and found results in reasonable agreement with those from HMI, with a return flow in the middle of the convection zone; however, they questioned the physicality of such flows, which do not obey the continuity equation. Rajaguru and Antia [95] analyzed four years of HMI data and found evidence of a return flow near the base of the convection zone and no strong evidence of a multiple-cell flow.

All in all, it is probably fair to say that there is still no reliable measurement of the meridional circulation in the deeper layers of the convection zone.

*3.2.2 Temporal variation*

Like the zonal flow, the meridional flow in the outer convection zone shows signs of being modulated by the solar cycle, with a pattern of flows into the activity belts (and by some reports outflows at slightly greater depth). This was observed for example, in ring-diagram [85] and time-distance [96] analysis of MDI data from the first half of Solar Cycle 23. More recently it has been studied in GONG and HMI data by Komm *et al* [97] (see Fig 9). This effect has been questioned as some kind of contamination of the measurements by active regions, but the results of Komm *et al* suggest that, as with the zonal torsional oscillation pattern, the flows change even before strong active regions appear.

## 4 Discussion

We hae described the major observational findings about the solar interior structure and dynamics in the last couple of decades. While the near-surface structure is clearly strongly influenced by solar-cycle variations as well as shorter-term variations less directly related to the activity cycle, the evidence for solar-cycle changes in the structure of the deep inner layers is still not plentiful. The rotation profile is well constrained except in the solar core, where we still need help from g-modes to establish the rotation rate. The solar-cycle variation of the zonal flows is well established and has been used to predict the behavior of the magnetic cycle on a timescale of about a year. There is also growing evidence for solar-cycle modulation of the meridional flow near the surface. Despite much effort in recent years, the nature of the meridional flow profile in the deep interior is still elusive.

In the near future, it will be interesting to see how the frequency variations and flows respond during the declining phase of Solar Cycle 24 and during Cycle 25. The past decade has given us ample evidence that the behaviour we see in one cycle may not repeat exactly in the next, which makes it important to continue the long-term observing programmes.

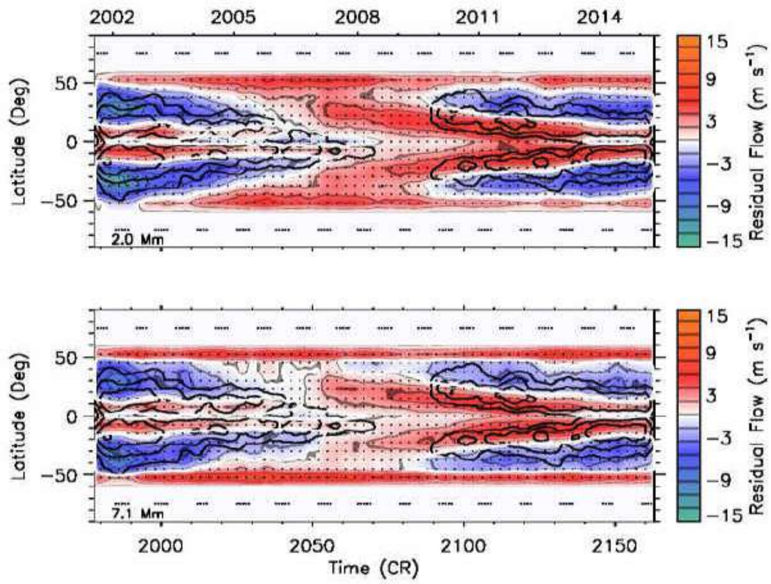


Fig 9. The residual meridional flow at two depths, from ring-diagram analysis of GONG data. The grey contours represent the magnetic field strength. Figure after Komm *et al* [97], courtesy of R Komm.

**Acknowledgements**

This work utilizes data obtained by the Global Oscillation Network Group (GONG) program, managed by the National Solar Observatory, which is operated by AURA, Inc. under a cooperative agreement with the National Science Foundation. The data were acquired by instruments operated by the Big Bear Solar Observatory, High Altitude Observatory, Learmonth Solar Observatory, Udaipur Solar Observatory, Instituto de Astrof´ısica de Canarias, and Cerro Tololo Interamerican Observatory. MDI data provided by the SOHO/MDI consortium. SOHO is a project of international cooperation between ESA and NASA. HMI data courtesy of NASA/SDO and the HMI science team. NSO/Kitt Peak data used here were produced cooperatively by NSF/NOAO, NASA/GSFC, and NOAA/SEL; SOLIS data are produced cooperatively by NSF/NSO and NASA/LWS.

The magnetic butterfly map used in Figs 5 and 3 was made from data kindly prepared by Dr Rudi Komm.

Figs 1 and 9 were kindly provided by Prof Sarbani Basu and Dr Rudi Komm, respectively.

The author acknowledges computing support from the National Solar Observatory. This review has made use of NASA's Astrophysics Data System.

**References**

1. Harvey J W, Hill F, Hubbard R, Kennedy J R, Leibacher J W, Pintar J A, Gilman P A, Noyes R W, Title A M, Toomre J, Ulrich R K, Bhatnagar A, Kennewell J A, Marquette W, Patron J, Saa O, Yasukawa E, *Science*, 272 (1996)1284-1286.
2. Scherrer P H, Bogart R S, Bush R I, Hoeksema J T, Kosovichev A G, Schou J, Rosenberg W, Springer L, Tarbell T D, Title A, Wolfson C J, Zayer I, MDI Engineering Team, *Sol Phys*, 162(1995)129-188.
3. Scherrer P H, Schou J, Bush R I, Kosovichev A G, Bogart R S, Hoeksema J T, Liu Y, Duvall T L, Zhao J, Title A M, Schrijver C J, Tarbell T D, Tomczyk S, *Sol Phys*, 275(2012)207-227.

4. Chaplin W J, Elsworth Y, Howe R, Isaak G R, McLeod C P, Miller B A, van der Raay H B, Wheeler S J, New R, *Sol Phys*, 168(1996)1-18.
5. Hale S J, Howe R, Chaplin W J, Davies G R, Elsworth Y P, *Sol Phys*, 291( 2016)1-28.
6. Gabriel A H, Grec G, Charra J, Robillot J-M, Cortes T R, Turck-Chieze S, Bocchia R, Boumier P, Cantin M, Cespedes E, Cougrand B, Cretolle J, Dame L, Decaudin M, Delache P, Denis N, Duc R, Dzitko H, Fossat E, Fourmond J-J, García R A, Gough D, Grivel C, Herreros J M, Lagardere H, Moalic J-P, Pallé P L, Petrou N, Sanchez M, Ulrich R, van der Raay H B, *Sol Phys*, 162(1995)61-91.
7. Basu S, Chaplin W J, Elsworth Y, New R, Serenelli A M, *Astrophys J*, 699(2009)1403-1417.
8. Schmitt J R, Basu S, *Astrophys J*, 80 (2015)123.
9. Christensen-Dalsgaard J, Dappen W, Ajukov S V, Anderson E R, Antia H M , Basu S, Baturin V A, Berthomieu G, Chaboyer B, Chitre S M, Cox A N, Demarque P, Donatowicz J, Dziembowski W A, Gabriel M, Gough D O, Guenther D B, Guzik J A, Harvey J W, Hill F, Houdek G, Iglesias C A, Kosovichev A G, Leibacher J W, Morel P, Proffitt C R, Provost J, Reiter J, Rhodes E J (Jr), Rogers F J, Roxburgh I W, Thompson M J, Ulrich R K, *Science* 272(1996)1286-1287.
10. Bahcall J N, Pinsonneault M H, Basu S, *Astrophys J*, 555(2001)990-1012.
11. Asplund M, Grevesse N, Sauval A J, in Cosmic Abundances as Records of Stellar Evolution and Nucleosynthesis, (eds) T G Barnes III and F N Bash, *Astron Soc Pac Conf Ser*, 336(2005)25-38.
12. Bahcall J N, Basu S, Pinsonneault, M, Serenelli A M, *Astrophys J*, 618(2005)1049-1056.
13. Basu S, Antia H M, *Phys Rep*, 457(2008)217-283.
14. Woodard M F, Noyes R W, *Nature*, 318(1985)449-450.
15. Pallé P L, Regulo C, Roca Cortes T, *Astron Astrophys*, 224(1989)253-258.
16. Elsworth Y, Howe R, Isaak G R, McLeod C P, New R, *Nature*, 345(1990)322-324.
17. Libbrecht K G, Woodard M F, *Nature*, 345(1990)779-782.
18. Antia H M , Basu S, Hill F, Howe R, Komm R W, Schou J, *Mon Not Royal Astron Soc*, 327(2001)1029-1040.
19. Howe R, Komm R W, Hill F, *Astrophys J*, 580(2002)1172-1187.
20. Hindman B, Haber D, Toomre J, Bogart R, *Sol Phys*, 192(2000)363-372.
21. Rajaguru S P, Basu S, Antia H M, *Astrophys J*, 563(2001)410-418.
22. Elsworth Y, Howe R, Isaak G R, McLeod C P, Miller B A, New R, Speake C C, Wheeler S J, *Astrophys J*, 434 (1994)801-806.
23. Campbell W R, Roberts B, *Astrophys J*, 338(1989)538-556.
24. Jain R, Roberts B, *Sol Phys*, 152(1994)261-266.
25. Bogdan T J, Zweibel E G, *Astrophys J*, 298 (1985) 867-875.
26. Foullon C, Roberts B, *Astron Astrophys*, 439(2005)713-726.
27. Roberts B, Campbell W R, *Nature*, 323(1986)603-605.
28. Dziembowski W A, Goode P R, *Astrophys J*, 625(2005)548-555.
29. Basu S, Broomhall A -M, Chaplin W J, Elsworth Y, *Astrophys J*, 758(2012)43.
30. Salabert D, García R A, Turck-Chieze S, *Astron Astrophys*, 578(2015)A137.
31. Fletcher S T, Broomhall A -M, Salabert D, Basu S, Chaplin W J, Elsworth Y, García R A, New R, *Astrophys J Lett*, 718(2010)L19-L22.
32. Lefebvre S, Kosovichev A G, *Astrophys J Lett*, 633(2005)L149-L152.
33. Rabello-Soares M C, *Astrophys J*, 745(2012)184.
34. Gizon L, Schunker H, Baldner C S, Basu S, Birch A C, Bogart R S, Braun D C, Cameron R, Duvall T L, Hanasoge S M, Jackiewicz J, Roth M, Stahn T, Thompson M J, Zharkov S, *Space Sci Rev*, 144(2009)249-273.
35. Basu S, Mandel A, *Astrophys J Lett*, 617(2004)L155-L158.
36. Verner G A, Chaplin W J, Elsworth Y, *Astrophys J Lett*, 640(2006)L95-L98.

37. Christensen-Dalsgaard J, Monteiro M J P F G, Rempel M, Thompson M J, *Mon Not Royal Astron Soc*, 414(2011) 1158-1174.
38. Eff-Darwich A, Korzennik S G, Jiménez-Reyes S, Pérez Hernández F, *Astrophys J*, 580(2002)574-578.
39. Baldner C S, Basu S, *Astrophys J*, 686(2008)1349-1362.
40. Schou J, Christensen-Dalsgaard J, Thompson M J, *Astrophys J*, 433(1994)389-416.
41. Pijpers F P, Thompson M J, *Astron Astrophys Lett*, 262(1992)L33-L36.
42. Pijpers F P, Thompson M J, *Astron Astrophys*, 281(1994)231-240.
43. Schou J, Antia H M, Basu S, Bogart R S, Bush R I, Chitre S M, Christensen-Dalsgaard J, Di Mauro M P, Dziembowski W A, Eff-Darwich A, Gough D O, Haber D A, Hoeksema J T, Howe R, Korzennik S G, Kosovichev A G, Larsen R M, Pijpers F P, Scherrer P H, Sekii T, Tarbell T D, Title A M, Thompson M J, Toomre J, *Astrophys J*, 505(1998)390-417.
44. Howe R, *Liv Rev Sol Phys*, 6(2009)1.
45. Eff-Darwich A, Korzennik S G, Jiménez-Reyes S J, *Astrophys J*, 573(2002)857.
46. Chaplin W J, Sekii T, Elsworth Y, Gough D O, *Mon Not Royal Astron Soc*, 355(2004)535.
47. Eff-Darwich A, Korzennik S G, *Sol Phys*, 287(2013)43-56.
48. García R A, Turck-Chièze S, Jiménez-Reyes S J, Ballot J, Pallé P L, Eff-Darwich A, Mathur S, Provost J, *Science*, 316(2007)1591-1593.
49. Brown T M, Christensen-Dalsgaard J, Dziembowski W A, Goode P, Gough D O, Morrow C A, *Astrophys J*, 343 (1989)526-546.
50. Dziembowski W A, Goode P R, Libbrecht K G, *Astrophys J Lett*, 337(1989)L53-L57.
51. Basu S, Antia H M, *Mon Not Royal Astron Soc*, 287(1997)189-198.
52. Wilson P R, Burtonclay D, Li Y, *Astrophys J*, 457(1996)440.
53. Corbard T, Berthomieu G, Provost J, Morel P, *Astron Astrophys*, 330(1998)1149-1159.
54. Miesch M S, *Living Rev Sol Phys*, 2(2005)1.
55. Gilman P A, Howe R, in Local and Global Helioseismology: the Present and Future, (ed) H Sawaya- Lacoste, ESA Special Publication, 517(2003)283-285.
56. Howe R, Christensen-Dalsgaard J, Hill F, Komm R, Schou J, Thompson M J, *Astrophys J*, 634(2005)1405-1415.
57. Corbard T, Thompson M J, *Sol Phys*, 205(2002)211-229.
58. Gilman P A, Foukal P V, *Astrophys J*, 229(1979)1179-1185.
59. Barekat A, Schou J, Gizon L, *Astron Astrophys*, 570(2014)L12.
60. Howard R, Labonte B J, *Astrophys J Lett*, 239(1980)L33-L36.
61. Kosovichev A G, Schou J, *Astrophys J Lett*, 48(1997)L207-L210.
62. Howe R, Komm R, Hill F, *Sol Phys*, 192(2000)427-435.
63. Howe R, Christensen-Dalsgaard J, Hill F, Komm R W, Larsen R M, Schou J, Thompson M J, Toomre J, *Astrophys J Lett*, 533(2000)L163-L166.
64. Antia H M, Basu S, *Astrophys J*, 541(2000)442-448.
65. Vorontsov S V, Christensen-Dalsgaard J, Schou J, Strakhov V N, Thompson M J, *Science*, 296(2002)101-103.
66. Antia H M, Basu S, *Astrophys J Lett*, 559(2001)L67-L70.
67. Howe R, Komm R, Hill F, Ulrich R, Haber D A, Hindman B W, Schou J, Thompson M J, *Sol Phys*, 235(2006) 1-15.
68. Howe R, Rempel M, Christensen-Dalsgaard J, Hill F, Komm R, Larsen R M, Schou J, Thompson M J, *Astrophys J*, 649(2006)1155-1168.
69. Howe R, Christensen-Dalsgaard J, Hill F, Komm R, Schou J, Thompson M J, *Astrophys J Lett*, 701(2009)L87-L90.

70. Howe R, Hill F, Komm R, Christensen-Dalsgaard J, Larson T P, Schou J, Thompson M J, Ulrich R, *J Phys Conf Ser*, 271(2011)012074.
71. Howe R, Christensen-Dalsgaard J, Hill F, Komm R, Larson T P, Rempel M, Schou J, Thompson M J, *Astrophys J Lett*, 767(2013)L20.
72. Rempel M, *Astrophys J Lett*, 750(2012)L8.
73. Schuessler M, *Astron Astrophys Lett*, 94(1981)L17-L18.
74. Yoshimura H, *Astrophys J*, 247(1981)1102-1112.
75. Spruit H C, *Sol Phys*, 213(2003)1-21.
76. Howe R, Christensen-Dalsgaard J, Hill F, Komm R W, Larsen R M, Schou J, Thompson M J, Toomre J, *Science*, 287(2000)2456-2460.
77. Silverman S M, Shapiro R, *J Geophys Res*, 88(1983)6310-6316.
78. Richardson J D, Paularena K I, Belcher J W, Lazarus A J, *Geophys Res Lett*, 21(1994)1559-1560.
79. Paularena K I, Szabo A, Richardson J D, *Geophys Res Lett*, 22(1995)3001-3004.
80. Basu S, Antia H M, *Mon Not Royal Astron Soc*, 324(2001)498-508.
81. Howe R, Christensen-Dalsgaard J, Hill F, Komm R, Schou J, Thompson M J, Toomre J, *Adv Space Res*, 40(2007) 915-918.
82. Howe R, Komm R, Hill F, Christensen-Dalsgaard J, Larson T P, Schou J, Thompson M J, Toomre J, *J Phys Conf Ser*, 271(2011)012075.
83. Hill F, *Astrophys J*, 333(1998)996-1013.
84. Duvall T L (Jr), Jefferies S M, Harvey J W, Pomerantz M A, *Nature*, 362(1993)430-432.
85. Haber D A, Hindman B W, Toomre J, Bogart R S, Larsen R M, Hill F, *Astrophys J*, 570(2002)855-864.
86. González Hernández I, Komm R, Hill F, Howe R, Corbard T, Haber D A, *Astrophys J*, 638(2006)576-583.
87. Zaatri A, Komm R, González Hernández I, Howe R, Corbard T, *Sol Phys*, 236(2006)227-244.
88. Zhao J, Nagashima K, Bogart R S, Kosovichev A G, Duvall T L ( Jr), *Astrophys J Lett*, 749(2012)L5.
89. Baldner C S, Schou J, *Astrophys J Lett*, 760(2012)L1.
90. Hathaway D H, *Astrophys J*, 760(2012)84.
91. Zhao J, Bogart R S, Kosovichev A G, Duvall T L (Jr), Hartlep T, *Astrophys J Lett* Lett, 774(2013)L29.
92. Schad A, Timmer J, Roth M, *Astrophys J Lett*, 778(2013)L38.
93. Kholikov S, Serebryanskiy A, Jackiewicz J, *Astrophys J*, 784(2014)145.
94. Jackiewicz J, Serebryanskiy A, Kholikov S, *Astrophys J*, 805(2015)133.
95. Rajaguru S P, Antia H M, *Astrophys J*, 813(2015)114.
96. Zhao J, Kosovichev A G, *Astrophys J*, 603(2004)776-784.
97. Komm R, González Hernández I, Howe R, Hill F, *Sol Phys*, 290(2015)3113-3136.


[*Received*: 15.1.2016; *accepted*:1.2.2016]